SINERGI Vol. 27, No. 3, October 2023: 309-318
http://publikasi.mercubuana.ac.id/index.php/sinergi
http://doi.org/10.22441/sinergi.2023.2.002

Optimization of Ultra-Wideband bandwidth for the design of microstrip monopole antennas using Defected Ground Structure and star-shaped patches

M. Darsono* **and Muhammad Rega**
Department of Electrical Engineering, Faculty of Engineering, Universitas Darma Persada, Indonesia

Abstract
This paper presents a design of a monopole microstrip antenna developed to support Ultra-wideband (3.1 -10.6 GHz) technology wireless communication systems. An antenna with minimalist dimensions operates on C-Band (wireless LAN) and X-Band (downlink satellite) frequencies. The antenna profile has a star shape patch on the top side and the use of the Defected Ground Structure (DGS) technique on the bottom side on RT DUROID substrate media. The design uses a simulation method using software and measurement tests on antenna prototypes to obtain parameters and antenna performance characteristics. The results of the measurement test, the bandwidth return loss < -10 dB has a difference of 40% (absolute) and 0.7% (Fractional) lower than the simulation when VSWR < 2. The radiation pattern forms an omnidirectional with a maximum directivity (Gain) of 5.18dBi with polarization vertical. Overall, the UWB monopole antenna design results have a low profile, compact, small size, and support mobile communication devices.

Keywords:
Antenna;
DGS;
Simulation;
Star Patch;
UWB;

Article History:
Received: September 6, 2022
Revised: February 20, 2023
Accepted: April 13, 2023
Published: October 2, 2023

Corresponding Author:
M. Darsono
Department of Electrical Engineering, Faculty of Engineering, Universitas Darma Persada, Indonesia
Email:
em_darsono@ft.unsada.ac.id

INTRODUCTION

The Antenna is a transducer designed to transmit or receive electromagnetic waves. Microstrip antennas have several advantages over conventional microwave antennas and are therefore widely used in many practical applications. On February 14, 2002, the Federal Communications Commission (FCC) amended the Part 15 rules which govern unlicensed radio devices to include the operation of Ultra-Wideband (UWB) devices. The FCC also allocated a bandwidth of 7.5GHz, i.e., from 3.1GHz to 10.6GHz to UWB applications, by far the largest spectrum allocation for unlicensed use the FCC has ever granted [1].

On December 15, 2004, the FCC issued its Second Report on UWB. This report allows for greater flexibility in the introduction of massive systems and devices that do not satisfy the definition of UWB technology. The amended legislation raises the peak emission power limits of wide-bandwidth devices to the same level as UWB devices in the three formerly unlicensed frequency bands, namely 5925-7250 MHz, 16.2-17.2 GHz, and 23.12-29 GHz. The availability of various services in narrow bands, such as Wireless LAN (WLAN) in the 5.15 to 5.85 GHz frequency region, X-region satellite downlink communication in the 7.1 to 7.6 GHz band, and Direct Communication, is the main issue with UWB antennas. Broadcast Satellite (DBS) operates in the frequency range of 11.7 to 12.5 GHz [2]. This results in electromagnetic interference problems in the UWB system [3, 4, 5].

UWB antennas have their charms and challenges in their design, according to the FCC, as a crucial component of the UWB system for wireless communication. As a crucial component of the UWB system, UWB antennas must have a compact size, lightweight, omnidirectional radiation pattern, and all other properties required

for UWB communication. As a result, there is a lot of interest in UWB technology research and development [6, 7, 8, 9].

Figure 1 UWB technology is appropriate for a wide range of applications, including communications, geo-location, positioning, and radar or sensor applications. The UWB system has advanced technologically for more than 40 years [2].

According to the Shannon-Hartley theorem, channel capacity in this system improves linearly as bandwidth increases and declines logarithmically when the signal-to-noise ratio (SNR) diminishes[10]. UWB technology's power is incredibly low and close to the noise level. As a result, the UWB system is power limited rather than band-restricted, as in the narrowband situation [2][11].

Several designs have been published to achieve the UWB frequency band, including the genetic algorithm, rectangular slot, round diamond, trident form bait, Quasi-self-free, Vivaldi antipodal, and many others. Ultra-wideband (UWB), a radio transmission method with a bandwidth surpassing 500MHz or at least 20% of the central frequency, is a game-changing approach for short-range high-bandwidth wireless communication [3][10].

The design of a compact ultra-wideband antenna printed on short-range radio devices plays an important part in current wireless communications in recent RF communications and remote sensing applications at radio, microwave, and terahertz frequencies. It is a short-range communications technique that uses no carriers and transfers data in the form of very short pulses [2][7].

Several works that have examined UWB microstrip antennas with the usage of star patches as slits or radiating patches have demonstrated good values with the support of specific grounding models [12][13]. The grounding model or technique is critical for obtaining a wide bandwidth. This criterion heavily relies on fractal geometry.

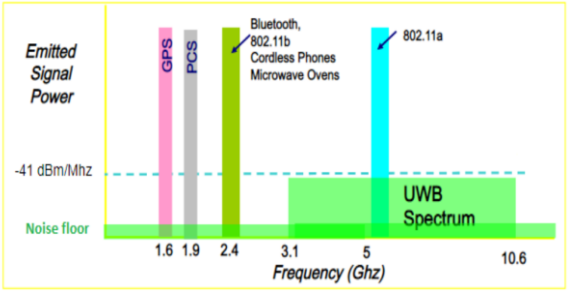

Figure 1. UWB versus other Radio Communication Systems [2]

Because fractals have non-integral dimensions, their propensity to fill space can be exploited to reduce antenna size [14]. The Method of the Moment analysis technique is used to optimize the outcomes by the design goal.

Microstrip antenna development that optimizes bandwidth can be performed through the use of techniques such as coupling proximity, Electromagnetic Band Gap (EBG), and Defected Ground Structure (DGS). In this study, the Electromagnetic Band Gap method, which is most commonly used at UWB frequencies, was used. At a specific frequency range, electromagnetic waves flow through the EBG, a periodic structure. On the ground plane construction, which is located at the center point, the notched band technique is applied. There are several methods for obtaining notch bands, including [14][15].

METHOD

The goal of the antenna design study is to create a simple, compact monopole antenna model that can operate in the UWB frequency spectrum. Using the Defected Ground Structure approach, obtain bandwidth optimization on the outcomes of the antenna design performance. Rogers-Corp RT DUROID 5880 substrates have a dielectric constant of 2.2, a thickness of 1.57mm, and a loss tangent of 0.002 [17].

In this study, a simulation model was run using moment application software to generate data from an overall antenna design. The goal of this research was to develop a microstrip antenna prototype that might be employed in wireless communication applications. The was created to be small and low-profile.

Antenna Design

Magnetic coupling technology is used in the antenna design of the EBG method's planar monopole antenna. The patch is built on the top layer of the substrate material in the opposite orientation as the ground plane. A particular star-shaped patch is made using two equilateral triangular patches.

In this, a star-shaped patch is made by fusing two triangles and rotating the angle by 180 degrees Figure 2 and Figure 3 [18].

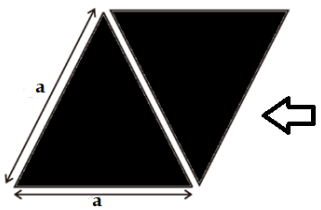

Figure 2. Triangular patch merge direction.

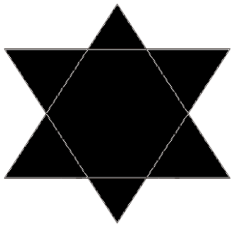

Figure 3. Star Patch

The basic shape of the star patch is formed by two triangular patches. Crosswise, the two triangular patches are 180 degrees apart. The equilateral triangular patch's shape can be determined by calculating the side lengths of the patch. The dimensional value determines the resonance substrate material's resonance frequency and dielectric constant are order modes in the Transverse Magnetic Wave Propagation (TM_{mn}) dominating mode. To determine the triangle's side length, apply (10) [17][18].

$$fr_{,mn} = \frac{2C}{3a\sqrt{\varepsilon_r \,,\mu_{eff}}}\sqrt{(n^2 + nm + m^2)} \quad (1)$$

Where fr is the relative dielectric constant of the material, eff is the dielectric material's effective permittivity, and fr is the resonant frequency in gigahertz. The speed of light is known as C (3 x 10^8 m/s). m = 1 and n = 0 in the case of the dominant mode (TM_{01}). As shown below, (2) is generated by lowering (1).

$$fr = \frac{2C}{3a\sqrt{\varepsilon_r}} \quad (2)$$

The following equation can be used to calculate the length of the triangle's side (a).

$$a = \frac{2C}{3f_r\sqrt{\varepsilon_r}} \quad (3)$$

The Star Patch Design

To determine the dimension value of the star patch, begin with an equilateral triangle-shaped patch. The operating range of UWB technology is 3.1 GHz to 10.6 GHz, which includes the C and X band frequencies. The resonance frequency (fr) or core frequency in the current study is 6.5 GHz, and the thickness (h) and dielectric constant (r) of the RT DUROID substrate are 1.57 mm and 2.2, respectively.

The side length of the triangle patch may be calculated using (3), and the result is 20 mm with a 60-degree angle on each side, as shown in Figure 4. The size of the star patch created by joining two equilateral triangles is seen in Figure 5.

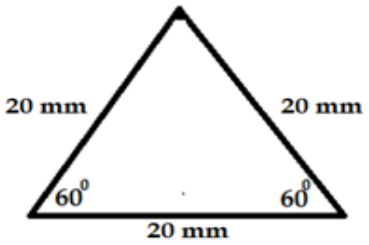

Figure 4. Triangular patch design

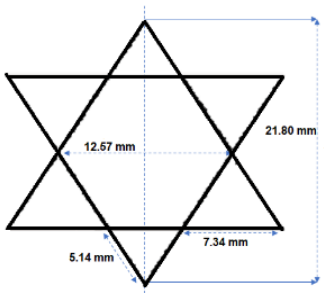

Figure 5. Star patch design

The diagonals of the star angles in the figure's two long sides are 12.57 mm and 21.8 mm. Two sides with lengths of 5.14 mm and 7.34 mm make up the corner of the triangle's junction.

Transmission Line

The microstrip transmission line is part of the antenna design element that functions as a power supply. The characteristic impedance of the microstrip transmission line can be calculated by analyzing the width of the line above the conductor's surface to the thickness of the substrate material. Figure 6 shows a profile of a microstrip transmission line depending on the value of the conductor width (*w*) and the thickness (*h*) of the substrate layer.

The medium or substrate type requirements define a microstrip transmission line's characteristic impedance (Zo). When the line width (w) to substrate thickness (h) ratio is greater than one (w/h > 1), then (4) can be used to calculate the characteristic impedance of the microstrip line [19][20].

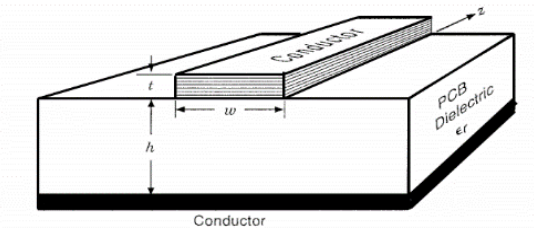

Figure 6. Microstrip line

$$Z_0 = \frac{[120\pi\sqrt{\varepsilon_{eff}}]}{\frac{h}{w}+1{,}393+0{,}667ln\left(1{,}444+\frac{w}{h}\right)} \quad (4)$$

Where Zo is the characteristic impedance in Ohms, eff is the material's relative dielectric constant, the substrate thickness is in meters, and w is the transmission line width in meters. Using (4), we can calculate that the transmission line width is 4.8 mm when the characteristic impedance (Zo) is 50Ω.

T-Junction Power Divider

For this research, the microwave transmission line as a power supply point to a loaded patch the T-junction power divider transmission line technique is used. T-junction microstrip is a technique of several types of microstrips in system telecommunication. A tapered microstrip is often found as a power separator also known as a splitter. The T-Junction power divider circuit shown in Figure 7 is a common design for microstrip antennas, where its performance is comparable to that of the three-port Wilkinson power divider [22]. The impedance value of the circuit is made up of three fundamental components: an input line (Zo), two output lines (Z_1), and (Z_2). There is no isolation between the output ports so other than at the T-junction [23].

The third transmission line impedance relationship of the T-junction power divider is as follows:

$$\frac{1}{z_0} = \frac{1}{z_1} + \frac{1}{z_2} + jB \quad (5)$$

Where Z0 is the input line's characteristic impedance, Z1, and Z2 are the output lines' characteristic impedances, and B is the reactance formed at the junction of the three lines. As a result, given an input impedance, the two output impedances can be matched to it. Furthermore, if B (imaginary side) is assumed to be zero, the value of the characteristic impedance of all becomes real. So, using (6), we established a relationship value for the three impedances of Zo, Z1, and Z2 [21][24].

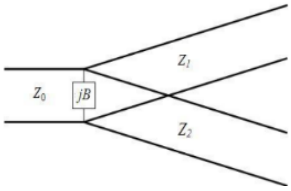

Figure 7. T-Junction Power Divider [23]

$$\frac{1}{z_0} = \frac{1}{z_1} + \frac{1}{z_2} \quad (6)$$

If the characteristic impedance (Zo) in (4) is 50Ω, then the output line impedances (Z_1 and Z_2) are 100Ω, respectively. As an outcome, the impedance of Z_1 and Z_2 has a 1.4 mm line width in the design of the microstrip transmission line.

Defected Ground Structure (DGS) Design

This technique merely denotes the placement of a "defect," which is sometimes considered an approximate approximation of an infinite, perfectly conducting current sink, in the plane's ground. Although the additional DGS perturbations modify the homogeneity of the ground plane, they do not cause it to be defective. The main component of DGS is a resonant gap or slot in the ground metal positioned precisely beneath a transmission line and angled for effective coupling to the line. DGS can be used as a filter in antennas operating in the UWB spectrum to reduce interference effects [14, 15, 24].

This is the most common usage of DGS for the Antenna because it can reduce side lobes in phase arrays, improve the performance of couplers and power dividers, and minimize the response to band signals for both transmit and receive [26][27]. This study employs different square-type forms as part of the DGS technique. The geometry of the DGS construction using a microstrip antenna's ground plane is depicted in Figure 8. Lg and Wg are the length and width of the ground plane on the DGS side of the construction, respectively. For a notch the same size as the ground plane's opening (Gp) [28, 29, 30].

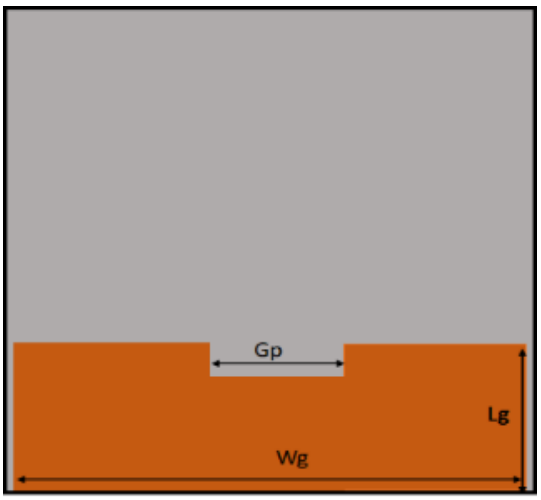

Figure 8. The ground plane's DGS

RESULTS AND DISCUSSION

Results for antenna design were obtained in this work using the simulation method. Two things may be seen from the simulation results: the antenna configuration's form and the Antenna's parameters. With a length and width of 40 millimeters for the first result, the substrate material has the smallest possible dimensions. The investigation of the Antenna's performance parameters follows, including measurements of bandwidth, VSWR, input impedance, radiation pattern, gain, and so forth.

Figure 9 shows the antenna design's front view structure, with the star patch and transmission line structure. Table 1 displays the results of the antenna design configuration in two components. The radiating patch, which is directly connected to the transmission line's source of power, is shown in the picture as a small antenna modeling design. The substrate material used for antenna modeling is required with a length (Ls) and width (Ws) of 40 mm x 40 mm. A transmission line with a characteristic impedance of 50 Ω is designed with a length (Lt) of 7. Millimeters and a width millimeters8 millimeters. Furthermore, the T-Junction power divider circuit has two output transmission lines with a gap (GD) of 11 millimeters with a line length (LD) of 10 millimeters and each has an impedance of 100 Ω(WD).

The lower layer of the ground plane is designed in Figure 10 using the DGS technique, and Table 2 explains the ground plane's dimensions. The ground plane area is limited to a width (Wg) of 38 millimeters and a length (Lg) of 12.2 millimeters.

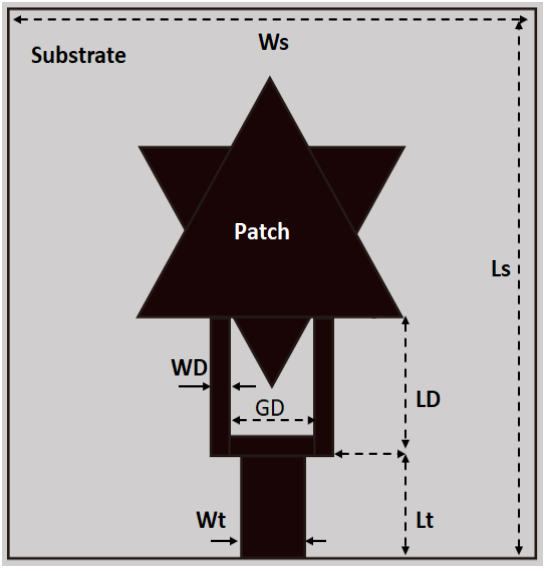

Figure 9. Design of Antenna top view.

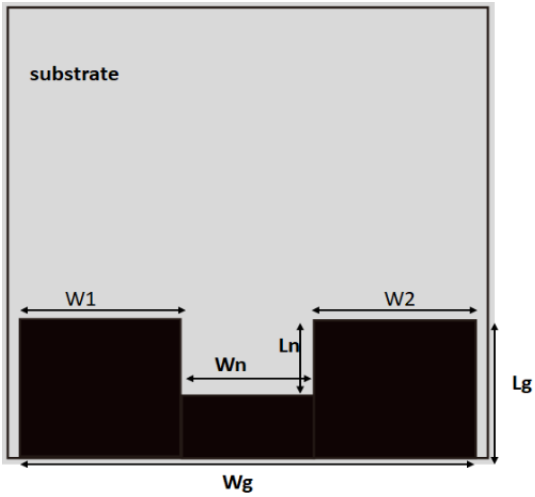

Figure 10. Design of Antenna bottom view.

Table 1. Dimension of Antenna top view.

Symbol	Dimension	Size (millimeter)
Ws	Width of Substrate	40
Ls	Length of Substrate	45
Wt	Width of the transmission line	4.8
Lt	Length of Transmission line	7.4
WD	Width of the output line power the power divider	1.4
GD	The gap between two output line power dividers	11
LD	Length of the output line power divider	10

Table 2. Dimension of Antenna bottom view

Symbol	Dimension	Size (millimeter)
Wg	The ground plane's width	38
Lg	The ground plane's length	12.2
W1=W2	Size of the ground's void between the left and rig.	13.5
Wn	Ground plane notch width	11
Ln	Ground plane notch length	6.5

The notch field has a slit width (Wn) of 11 millimeters and a length (Lp) of 5 millimeters, where the width of the slit to the edge (W1 = W2) of the ground plane is 13.5 millimeters each.

Parameters S11

The frequency limit on return loss, as shown in Figure 11 and Figure 12, is used to determine the bandwidth parameter S11. Figure 11 shows the simulation results of the return loss graph versus frequency. The bandwidth of return loss is below -10 dB from 2.1573 GHz (marker1) to 8.7247 GHz (marker4). The results of fractional bandwidth analysis are 1.2% and the absolute bandwidth is 6.5674 GHz. While the measurement results are shown in Figure 12, the graph of return loss on frequency shows the lowest frequency range is 5.84 GHz (marker 2)

and the highest frequency is 9.76 GHz (marker 3). The results of fractional bandwidth analysis are 0.5% and the absolute bandwidth is 3.92 GHz. Bandwidth optimization from simulation to measurement with a difference of 0.7% (fractional) or 2.647 GHz (absolute).

Bandwidth impedance matching can be seen in the VSWR (voltage standing wave ratio) value, where the value limit is 1 to 2. The simulation results and measurements of VSWR values can be seen in Figure 13 and Figure 14.

Figure 13 shows the VSWR graph versus the frequency of the simulation results, where impedance matching at the frequency 5.796 GHz when the VSWR is 1.0098 (marker 2) and at 8.161GHz when the VSWR is 1.2 (marker 3). While the results of the VSWR measurements are shown in Figure 14, where the impedance matches at the 5.84 GHz frequency when the VSWR is 1.147 (marker 2) and at the 9.76 GHz frequency when the VSWR is 1.8 (marker 3).

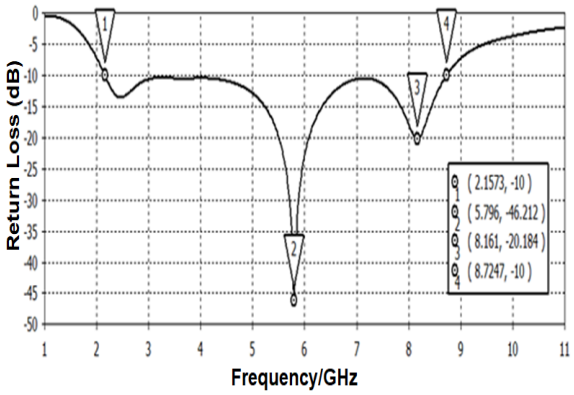

Figure 11. Return loss Versus Frequency of simulation result.

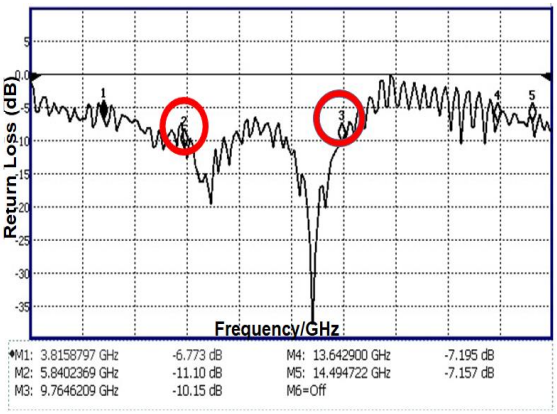

Figure 12. Return loss Versus Frequency of measurement result.

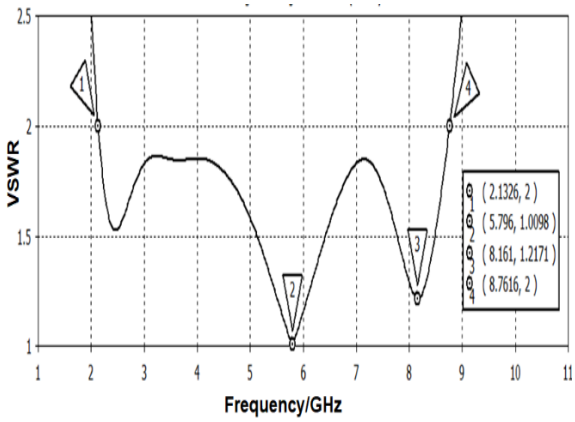

Figure 13. VSWR Versus Frequency of the simulation result.

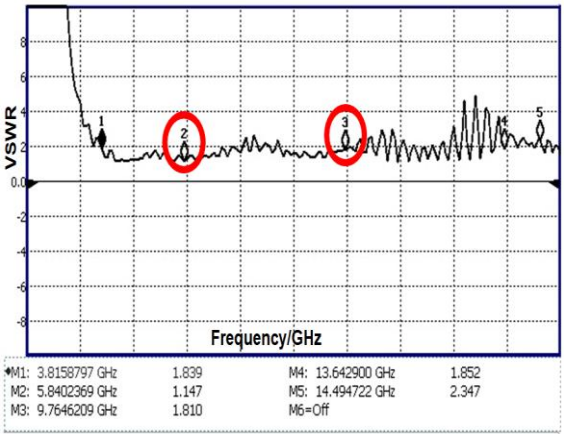

Figure 14. VSWR Versus Frequency of measurement result.

Radiation Pattern

Figure 15 and Figure 16 show the shape of the plane (theta) and angular (phi) radiation patterns normalized at the resonant frequencies of 5.796GHz and 8.161 GHz. The formed radiation obtained the maximum directivity (Gain) values of 2.61dBi and 5.18dBi. Figure 15 and Figure 16 The radiation polarization of each frequency takes the form of bidirectional (Main lobe directional) with the angle plane (*phi*) being 161^0 and 156^0, thus forming an omnidirectional radiation polarity.

The omnidirectional radiation polarization forms the polarization of the two resonant frequencies in the theta plane with two beam width angles. Figure 17 shows at the frequency of 5.796 GHz, the maximum beam width with a magnitude of 3dB is 84.5 degrees. Figure 18 shows the beam-width angle at the frequency of 8.161 GHz is 52.90 degrees.

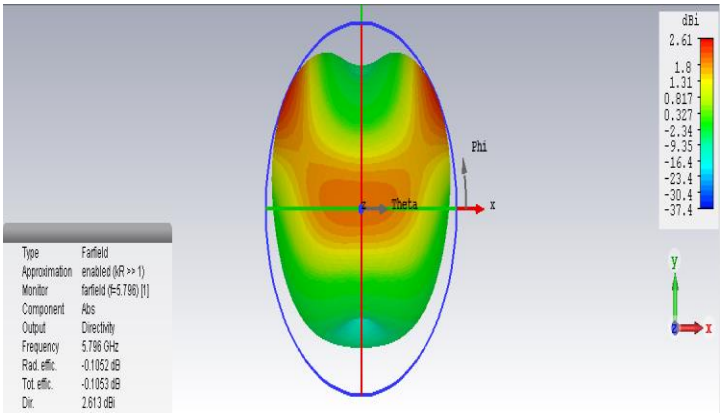

Figure 15. Radiation pattern at a frequency of 5.796 GHz

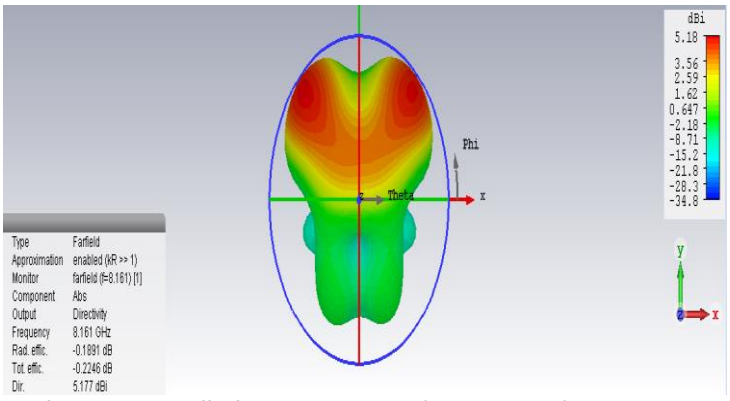

Figure 16. Radiation pattern at a frequency of 8.161 GHz

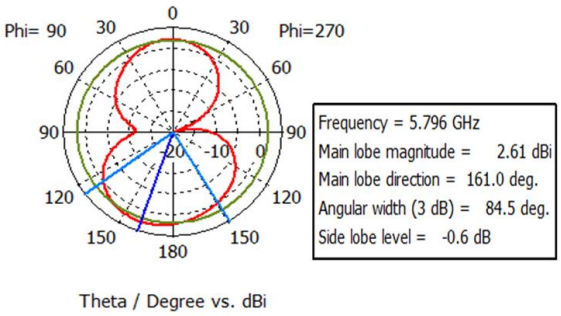

Figure 17. Far-field on the frequency of 5.796 GHz in the theta

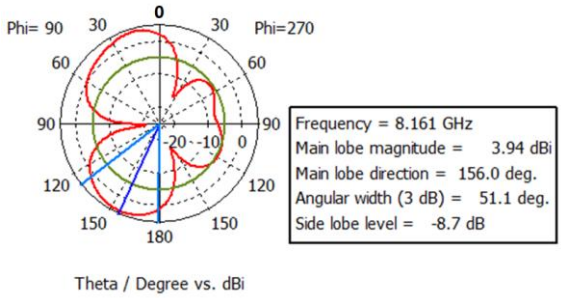

Figure 18. Far-field on the frequency of 8.161 GHz in the theta

Prototype Antenna

Figures 19(a) and 19(b) show the shape of the antenna prototype fabricated using the RT DUROID substrate material, which has dimensions of 40 x 40 millimeters. This prototype was built with the etching process. Figure 19(a) shows the front view of an antenna structure consisting of a patch and a power supply line with an attachment. Furthermore, Figure 19(b) shows the underside shape of the ground plane with the DGS technique.

Table 3 shows the antenna design performance resulting from the simulation and measurement methods. As a UWB monopole antenna, where the absolute bandwidth requirements are above 500MHz fractional above 0.2%. While the cut-off frequency range of the simulation and measurement results covers the C-Band and X-band spectrum areas. The antenna radiation pattern is omnidirectional with a beam width above 80 degrees with a maximum directivity (Gain) of 5.18dBi.

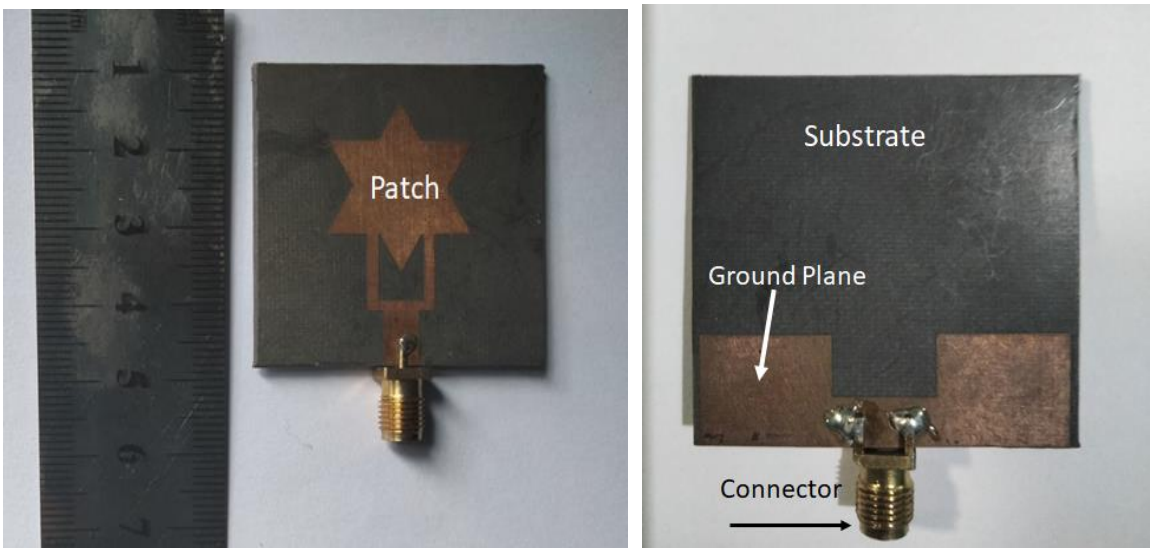

(a) (b)

Figure 19. (a) View (b) Bottom, Prototype of Antenna

.

Table 3. Performance of Antenna Design

Parameters	Simulation	Measurement
Bandwidth Absolut	6.5674 GHz	3.92 GHz
Bandwidth Fractional	1.2%	0.5%
Frequency Range	2.157 -8.724GHz	5.84-9.76GHz
VSWR max	< 2	1,8
Impedance	50Ω	50 Ω
Polarization	Vertical	NA
Radiation Pattern	omnidirectional	NA
Gain max	5.18dBi	NA
3dB Beam Width H-Plan	84.5 Degree	NA
3dB Beam Width E-Plan	52.90 Degree	NA

CONCLUSION

The result of minimalist dimensions and compact (40mm x 40mm) is an omnidirectional monopole antenna. Performance in operating in the UWB frequency region (3.1-10.6GHz), where the bandwidth of return loss <-10 dB and VSWR <2. The results of the bandwidth measurement test obtained were 40% (absolute) and 0.7% (fractional) smaller than the simulation. For applications, wireless communication support is measured in the working frequency range of Wireless LAN (5.15 to 5.85 GHz) C-Band and X-Band satellite downlink communications (7.1 to 7.6 GHz). The results of the overall antenna design support the development of UWB technology for high-speed network and data access.

ACKNOWLEDGMENT

Thank you to LP2MK, Darma Persada University, for funding this research, and to Muhammad Rega, a student, for helping with the simulation process. Hopefully, in the future, you will be enabled to conduct better research and contribute to technological developments.

REFERENCES

[1] NN, “Federal Communications Commission,” 2002. Accessed: Feb. 02, 2022. [Online]. Available: https://transition.fcc.gov/Bureaus/Engineering_Technology/Orders/2002/fcc02048

[2] A. Sarkar, S. Sultana, A. Paul, and M. M. Rashid, “Study on Ultra-Wideband (UWB) System and Its Applications,” *Journal of Bangladesh Electron*, vol. 18, no. 1–3, pp. 47-54, 2018.

[3] NN, “Characteristics of ultra-wideband technology.” *Rec. ITU-R*, SM.1755-0, pp. 1-20, 2006.

[4] M. Shi, L. Cui, H. Liu, M. Lv, and X. Sun, “A New UWB Antenna with Band-Notched Characteristic,” *Progress In Electromagnetics Research M*, vol. 74, pp. 201–209, 2018, doi: 10.2528/PIERM18081002

[5] Q. M. Hamza, S. M. Nabil and M. Hassan, "Microstrip Patch Antenna for Ultra-Wideband Applications," *2018 International Symposium on Advanced Electrical and Communication Technologies (ISAECT)*, Rabat, Morocco, 2018, pp. 1-4, doi: 10.1109/ISAECT.2018.8618854.

[6] X. Ling, “Ultra-Wideband Antenna and Design,” in *Ultra-Wideband - Current Status and Future Trends*, InTech, 2012. doi: 10.5772/47805.

[7] O. P. Kumar, P. Kumar, T. Ali, P. Kumar, and S. Vincent, “Ultrawideband Antennas: Growth and Evolution,” *Micromachines*, vol. 13, no. 1, Jan. 01, 2022. doi: 10.3390/mi13010060.

[8] J. Becker, D. Filipovic, H. Schantz, and S.-Y. Suh, “Ultra-Wideband Antennas,” *International Journal of Antennas and Propagation*, vol. 2008, ID: 731247, pp. 2, 2008, doi: 10.1155/2008/731247

[9] E. K. I. Hamad and A. H. Radwan, "Compact UWB antenna for wireless personal area networks," *2013 Saudi International Electronics, Communications and Photonics Conference*, Riyadh, Saudi Arabia, 2013, pp. 1-4, doi: 10.1109/SIECPC.2013.6551021.

[10] D. Xinzhong & S. R. Dueñas, “Design of a DS-UWB Transceiver,” *Ultra Wideband Communications: Novel Trends - System, Architecture and Implementation,* March, pp. 82, 2005.

[11] D. Coppens, A. Shahid, S. Lemey, B. Van Herbruggen, C. Marshall and E. De Poorter, "An Overview of UWB Standards and Organizations (IEEE 802.15.4, FiRa, Apple): Interoperability Aspects and Future Research Directions," in *IEEE Access*, vol. 10, pp. 70219-70241, 2022, doi: 10.1109/ACCESS.2022.3187410.

[12] M. Abu Nasr, M. K. Ouda, and S. O. Ouda, “Design of Star-Shaped Microstrip Patch Antenna for Ultra Wideband (UWB) Applications,” *International Journal of Wireless & Mobile Networks*, vol. 5, no. 4, pp. 65-73, Aug. 2013, doi: 10.5121/ijwmn.2013.5405.

[13] Y. Rahayu and I. A. Pohan, “Design of rectangular with 3 slot microstrip antenna for application lte 2.1 GHz,” *SINERGI*, vol. 22, no. 2, pp. 127-131, 2018, doi: 10.22441/sinergi.2018.2.009.

[14] S. Khade, M. Bhagat, S. Tompe, and S. Khatri, “Design of Star-Shaped Fractal

Antenna for Wireless Applications," vol. 134, no. 4, pp. 41-43, 2018, doi: 10.5120/ijca2016907913.
[15] M. K. Khandelwal, B. K. Kanaujia, and S. Kumar, "Defected ground structure: Fundamentals, analysis, and applications in modern wireless trends," *International Journal of Antennas and Propagation*, vol. 2017, 2017. doi 10.1155/2017/2018527.
[16] A. Kumar and K. V. Machavaram, "Microstrip filter with defected ground structure: A close perspective," *International Journal of Microwave and Wireless Technologies*, vol. 5, no. 5, pp. 589–602, 2013, doi: 10.1017/S1759078713000639.
[17] R. Corporation, "RT/duroid 5880LZ High Frequency Laminates Data Sheet," 2021. [Online]. Available: www.rogerscorp.com
[18] W. N. Najwa, W. Marzudi, Z. Z. Abidin, S. H. Dahlan, K. N. Ramli, and M. R. Kamarudin, "Performance of Star Patch Antenna on A Paper Substrate Materials," *ARPN Journal of Engineering and Applied Sciences*, vol. 10, no. 19, pp. 8606-8619, 2015, [Online]. Available: www.arpnjournals.com
[19] S. Sotyohadi, R. Afandi, and D. Rachmad Hadi, "Design and Bandwidth Optimization on Triangle Patch Microstrip Antenna for WLAN 2.4 GHz," in *MATEC Web of Conferences*, vol. 164, Apr. 2018, doi: 10.1051/matecconf/201816401042.
[20] K. Chang, I. Bahl and V. Nair, *RF and Microwave Circuit and Component Design for Wireless Systems*, vol. 63. Wiley, 2002.
[21] K. Chang, *RF and microwave wireless systems*, John Wiley & Sons, Inc., 2000
[22] C.-T. Chiang, U. Tunku, and A. Rahman Malaysia, "Ultra Wideband Power Divider Using Tapered Line," *Progress In Electromagnetics Researc*h, vol. 106, pp. 61-73, 2010, doi: 10.2528/PIER10061603
[23] L. J. Berens, "Design, Analysis, and Construction of an Equal Split Wilkinson Power Divider," Master Thesis, Marquette University, US, 2012.
[24] S. Johnson, "Microstrip and CPW Power Divider Design PathWave Advanced Design System (ADS)," 2022
[25] A. Nouri and G. R. Dadashzadeh, "A compact UWB band-notched printed monopole antenna with defected ground structure," *IEEE Antennas Wirel. Propag. Lett.*, vol. 10, pp. 1178–1181, 2011, doi: 10.1109/LAWP.2011.2171312.
[26] Rahul Sharma and Dr A. N. Mishara, "Analysis and Design of Microstrip Antenna with Defected Ground Structure for UWB Application," *International Journal of Engineering Research & Technology*, vol. V5, no. 01, pp. 810–812, 2016, doi: 10.17577/ijertv5is010636.
[27] D. Rusdiyanto, C. Apriono, D. W. Astuti, and M. Muslim, "Bandwidth and Gain Enhancement of Microstrip Antenna Using Defected Ground Structure and Horizontal Patch Gap," *SINERGI*, vol. 25, no. 2, pp. 153-158, 2021, doi: 10.22441/sinergi.2021. 2.006.
[28] M. Hussain *et al.*, "Bandwidth and Gain Enhancement of a CPW Antenna Using Frequency Selective Surface for UWB Applications," *Micromachines*, vol. 14, no. 3, pp. 591, 2023, doi: 10.3390/mi14030591.
[29] K. Mandal, "A Review on Printed Monopole Antenna for UWB Applications," *International Journal of Advanced Research in Computer and Communication Engineering*, vol. 4, no. 2, pp. 508-510, 2015, doi: 10.17148/IJARCCE.2015.412145.
[30] A. Firdausi, L. Damayanti, G. P. N. Hakim, U. Umaisaroh and M. Alaydrus, " Design of A Dual-Band Microstrip Antenna for 5G Communication," *Journal of Integrated and Advanced Engineering (JIAE)*, vol. 1, no. 1, pp. 65-72, 2021, doi: 10.51662/jiae.v1i1